Sensors and Actuators B 255 (2018) 3227–3234

Contents lists available at ScienceDirect

Sensors and Actuators B: Chemical

journal homepage: www.elsevier.com/locate/snb

Research Paper

Improved glucose label-free biosensor with layer-by-layer architecture and conducting polymer poly(3,4-ethylenedioxythiophene)

Melinda David [a,b], Madalina M. Barsan [a], Christopher M.A. Brett [a], Monica Florescu [b,*]

[a] Department of Chemistry, Faculty of Sciences and Technology, University of Coimbra, 3004-535 Coimbra, Portugal
[b] Faculty of Medicine, Transilvania University of Brasov, 500019 Brasov, Romania

ARTICLE INFO

Article history:
Received 7 February 2017
Received in revised form 30 August 2017
Accepted 21 September 2017
Available online 22 September 2017

Keywords:
Layer-by-layer
Poly(3,4-ethylenedioxythiophene) (PEDOT)
Enzymes
Electrochemical biosensors
Surface plasmon resonance spectroscopy

ABSTRACT

Layer-by-layer (LbL) self-assembly has been used for the development of a new glucose label-free biosensor. Glucose oxidase (GOx) was incorporated in a multilayer film on a gold electrode, previously modified with a film of the conducting polymer poly(3,4-ethylenedioxythiophene) (PEDOT), by electropolymerization, for better conductivity. Multilayer films, containing the enzyme and nitrogen doped graphene (NG) dispersed in the biocompatible positively-charged polymer chitosan {chit^{+}(NG + GOx)}, together with the negatively charged polymer poly(styrene sulfonate), PSS^{-}, were assembled. Cyclic voltammetry and electrochemical impedance spectroscopy were used for characterization of the biosensor architectures. The LbL film growth was monitored by Surface Plasmon Resonance Spectroscopy in order to evaluate the interactions involved in the biomolecule immobilization. Atomic force microscopy and scanning electron microscopy imaging show the morphological structure of the multilayer film modified electrode. The analytical properties of the glucose biosensor were determined by fixed potential amperometry and showed a substantial improvement in biosensor sensitivity in the presence of PEDOT. The biosensor operates at a low potential of −0.2 V vs. Ag/AgCl, with a sensitivity of 237 μA cm^{-2} mM^{-1} and a detection limit of 41 μM. The biosensor applicability was evaluated by measuring glucose content in wines obtained from Romanian grapes (*Vitis vinifera*).

1. Introduction

The performance of an enzyme-based biosensor depends on the specificity and sensitivity of the biological reaction, as well as on the stability of the entrapped enzyme [1]. In comparison with other immobilization techniques, layer-by-layer (LbL) self-assembled multilayers are architectures with a very precise control of composition, thickness and stability [2], being a mild entrapment method for enzyme immobilization, based on the adsorption of aqueous solutions onto solid supports [3]. An often-used LbL deposition method is the alternate dipping of the substrate into polyelectrolytes carrying surface charges of opposite signs, or hydrogen bond donors and acceptors [4]. Such configurations allow direct electron transfer between the enzyme active centre and the electrode surface [5]. A further advantage of this technique is the small amount of materials used.

For enzyme biosensors, LbL makes use of polyelectrolytes which are alternated with oppositely charged layers containing the enzyme. For example, positively-charged poly(ethyleneimine) PEI [6] or chitosan [7,8], can be alternated with polyanions such as poly(styrene sulfonate) PSS [9] or poly(vinyl sulfonate) PVS [10]. Furthermore, conducting polymers present dual advantages by binding the enzyme and facilitating electron transfer. The mechanism of conduction in these polymers is very complex and can be influenced by a variety of factors such as chain length and charge transfer to adjacent molecules [11]. Poly(3,4-ethylenedioxythiophene) PEDOT is a widely used conducting polymer. It has been demonstrated to have a high electrochemical stability, low energy band gap, good conductivity and enzyme immobilization capacity along with biocompatibility [12].

Based on the results obtained in our previous work [13] where we successfully dispersed glucose oxidase (GOx) together with nitrogen doped graphene (NG) in the positively-charged chitosan, forming a multilayer film alternating with the negatively-charged

* Corresponding author at: Colina Universitatii nr 1, Building C, room CI30, 500068 Brasov, Romania.
E-mail address: florescum@unitbv.ro (M. Florescu).

https://doi.org/10.1016/j.snb.2017.09.149
0925-4005/

poly(styrene sulfonate) PSS, we now added PEDOT to the structure. Chitosan is employed for enzyme immobilization through covalent linkage for which the PEDOT film offers an excellent substrate. Both PEDOT and chitosan show good biocompatibility, but the main goal of the work was to significantly improve biosensor performance by overcoming the poor conductivity of chitosan [14] by using nanomaterials in combination with PEDOT [15]. Graphene shows an ambipolar electric field effect, its electron mobility remaining high due to the charge carriers, which can be continuously tuned between electrons and holes [16]. Nitrogen doping of graphene by thermal annealing in the presence of ammonia leads to an improvement in its conductivity [17].

The self-assembly of the layers was monitored and characterized electrochemically by means of cyclic voltammetry (CV) and electrochemical impedance spectroscopy (EIS). Surface Plasmon Resonance (SPR) was employed to monitor the interaction between the layers of the LbL assembly. SPR permits real-time analysis of molecular interactions offering information simultaneously about the electrochemical and optical properties of thin films [18]. SPR is a good analytical tool, since it is very sensitive to small changes in the refractive index, which varies with the change of mass on the biosensor surface [19]. The physical appearance and surface characteristics of the assembled layers were monitored by scanning electron microscopy (SEM) and atomic force microscopy (AFM). The influence of incorporation of PEDOT in the biosensor architecture on analytical properties, sensitivity, stability and repeatability was assessed. In order to demonstrate the biosensor's applicability, it was used to determine the concentration of glucose in *Vitis vinifera* extracts.

2. Materials and methods

2.1. Materials

All reagents used were of analytical grade. Chitosan (low molecular weight), minimum 85% degree of deacetylation (due to its higher positive charge density), monobasic and dibasic sodium phosphate, sodium poly(styrene sulfonate) (NaPSS), 3,4-ethylenedioxythiophene (EDOT) solution, glucose oxidase (GOx) from Aspergillus niger (with a concentration of 17.3 U/mg), glucose, ascorbic acid, catechol, citric acid, dopamine, fructose, oxalic acid, uric acid and sucrose were all purchased from Sigma-Aldrich, Germany. N-doped graphene (NG) was prepared according to the procedure described in [17] and was a gift from Prof. X. Sun, University of Western Ontario, Canada. The grape extracts were obtained from Romanian white grapes. Three samples of white wine obtained from Romanian grapes freshly squeezed and left to ferment: E1, E2 and E3. All experiments were performed in neutral sodium phosphate buffer 0.1 M NaPB pH = 7.0. The aqueous glucose solution was prepared 24 h prior to measurements, in order to obtain its biologically active form (β-D-glucose). Millipore Milli-Q nanopure water (resistivity ≥ 18 MΩ cm) was used for the preparation of all solutions. All experiments were performed at room temperature (22 ± 1 °C) and all electrodes were kept in buffer solution at ~4 °C in a refrigerator in between measurements.

2.2. Instrumentation

All electrochemical measurements were carried out in a conventional electrochemical cell containing three electrodes. Gold bulk disc electrodes in a Teflon sheath, area 0.785 mm^2 (eDAQ Pty. Ltd.) were used as working electrodes for electrochemical studies, with a platinum foil as counter electrode and a silver/silver chloride electrode Ag/AgCl (3 M KCl) as reference.

Chrono-amperometric, electrochemical impedance and voltammetric measurements were performed by using a PalmSens3 electrochemical sensor interface (Palm Instruments BV, The Netherlands) controlled with PSTrace 4.8 software. For impedance measurements, an rms perturbation of 10 mV was applied over the frequency range 50 kHz–0.1 Hz, with 10 frequency values per frequency decade. The spectra were recorded at a potential of −0.2 V vs Ag/AgCl, and plotted in the form of complex plane diagrams and fitted to equivalent electrical circuits using EIS Spectrum Analyzer 1.0 software (http://www.abc.chemistry.bsu.by/vi/analyser/).

A SPR Navi 200 System and planar gold SPR discs from BioNavis LTD, Finland, were used to evaluate the interactions involved in biomolecule immobilization on surfaces, with the software packages for data acquisition and analysis SPR Navi Control and SPR Navi DataViewer. Bionavis 200 is based on the Kretschmann configuration in which a polarised, collimated light beam undergoes total internal reflection at a glass/thin-metal-film/dielectric interface. It is equipped with 2 lasers with wavelength of 670 nm. The sensor surface is formed by a glass chip coated with a 50 nm thin gold layer which produces the SPR effect. Before the SPR experiment, the Au thin film surface was covered with a thin film of PEDOT, following the protocol described below (Section 2.3, LbL biosensor architecture). The functionalized gold surface mounted on the SPR equipment was used as working electrode together with platinum and silver wires in a 100 μl electrochemical-SPR cell and connected to the electrochemical sensor interface PalmSens3 (Palm Instruments BV, The Netherlands) controlled by PSTrace 4.8 software. The working temperature was set at 21 °C.

Scanning electron microscopy (SEM) images were taken with a SU-70 by Hitachi. The conditions for morphological investigations of the sensor surface were: field-free mode, 5 kV accelerating voltage, and working distance in the range of 13.7–19.4 mm. Atomic force microscopy (AFM) was performed with a NTEGRA Prima by NT-MDT, for 2D and 3D topographic images. A polysilicon cantilever (HA_NC) with mono-crystal silicon tip coated by a 20 nm gold layer was used. The tip length is ~10 μm and the cantilever resonance frequency is 235 kHz.

2.3. LbL biosensor architecture

First, a PEDOT film was electrodeposited on the clean Au surface from an aqueous solution containing 0.1 M NaPSS and 10 mM EDOT. Preparation of the solution of 0.1 M NaPSS and 10 mM EDOT involved continuous stirring and heating, until a homogeneous solution was obtained [20]. The electrodes were then immersed in this solution and EDOT was polymerized by potential cycling, in the potential range −0.6 to 0.8 V, at a scan rate of 50 mV s^{-1}. Electrochemical polymerization of EDOT:PSS causes the monomer to deposit and oxidize on the gold electrode surface, forming insoluble polymer chains with a well-defined surface morphology. PEDOT:PSS formed a light grey, porous, negatively charged film (due to SO_3^-) on the electrode surface, facilitating deposition of a positively-charged layer. The amino groups in chitosan make possible both cross-linking to the porous PEDOT:PSS film, and electrostatic binding to its negatively charged SO_3^- groups. LbL self-assembly was then carried out on top of the PEDOT:PSS film making use of the electrostatic interactions between the positively-charged chitosan and negatively-charged PSS. NG 0.05% (w/v) was used as received and homogeneously dispersed together with the enzyme GOx in 1% (w/v) chitosan dissolved in 1% (v/v) acetic acid, designated chit$^+$(NG + GOx). The PEDOT-modified electrodes were immersed in this solution for 20 min, rinsed with water and dried in a nitrogen stream. They were then immersed in 1% PSS aqueous solution for 20 min, rinsed with water and dried in the same way. These steps were repeated for further bilayer deposition.

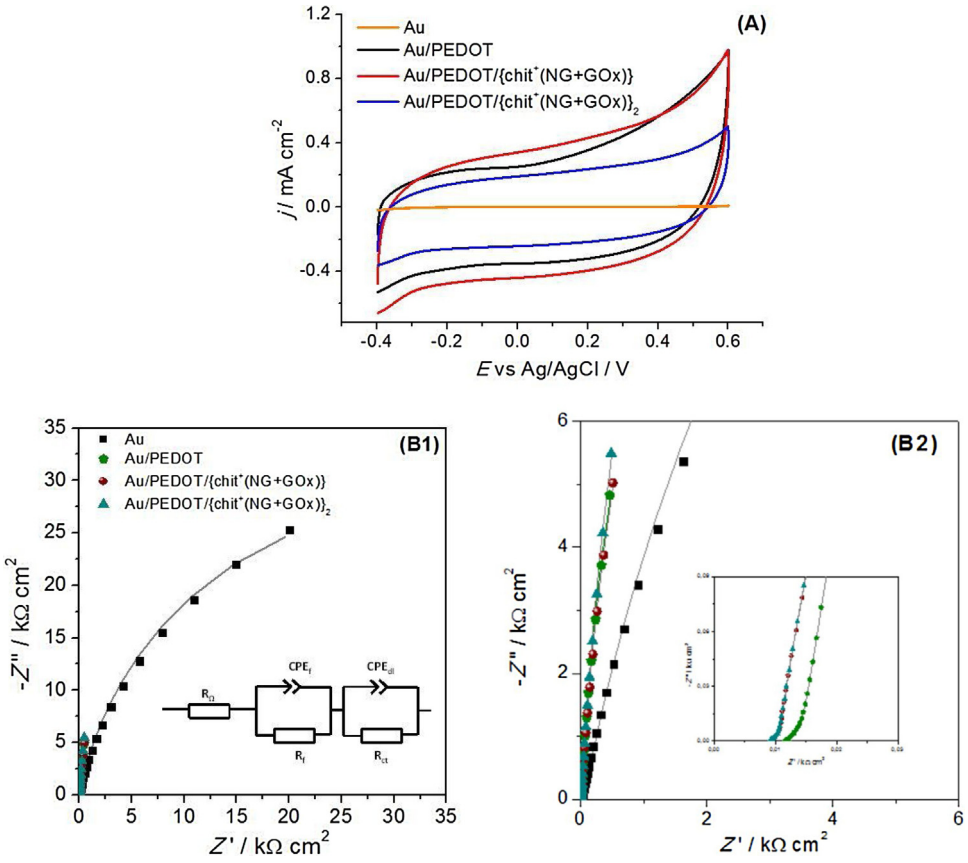

Fig. 1. Electrochemical measurements for Au, Au/PEDOT, Au/PEDOT/{chit$^+$(NG + GOx)}$_{n=1,2}$ in 0.1 M NaPB pH 7.0: (A) Cyclic voltammograms, $\upsilon = 50$ mV s^{-1}. (B1) Complex plane plots at −0.2 V vs. Ag/AgCl with the equivalent circuit used to fit the spectra; (B2) magnifications of (B1) in the high frequency region.

For SPR measurements, experiments were performed in a closed electrochemical cell of volume 100 μl, where all solutions were introduced by injection. Since SPR is a very sensitive tool for monitoring thin layer deposition, all solutions were used with half of their usual concentration (0.5%) and NG was left out in order to avoid clogging of the tubing and because it does not play any role in the electrostatic adsorption process. As shown in previous work [21], a higher concentration of chitosan may decrease the capacitive currents since it is not conductive [22]; therefore, the architecture of a maximum of two enzymatic layers i.e. Au/PEDOT/{chit$^+$(GOx)/PSS$^-$/chit$^+$(GOx)} was used for all SPR measurements.

3. Results and discussion

3.1. Electrochemical biosensor characterization

Electrochemical measurements, cyclic voltammetry (CV) and electrochemical impedance spectroscopy (EIS), were carried out at Au, Au/PEDOT, Au/PEDOT/{chit$^+$(NG + GOx)}$_{n=1,2}$ in 0.1 M NaPB pH = 7.0, and are shown in Fig. 1.

CV monitoring, Fig. 1A, offers an insight of both LbL adsorption and the change of the capacitance values on addition of each layer due to adsorption of the charged species. The first PSS layer was found not to change the characteristics of the first adsorbed chitosan layer [13]. The PSS layer is composed of small conducting molecules, too thin to give rise to an additional diffusion barrier in the biosensor architecture.

Capacitance values were calculated in the non-faradaic region at 0.1 V. The PEDOT layer led to a substantial increase in the capacitance from 10.2 μF cm^{-2} for bare Au, up to 5.9 mF cm^{-2} which was further increased by the first chit$^+$(NG + GOx) layer, up to 8.0 mF cm^{-2}. On addition of the second enzymatic layer, the capacitance started to decrease (4.3 mF cm^{-2}), that can be attributed to the non-conductive nature of chitosan. Electrochemical impedance spectroscopy allows the characterization of surface phenomena, providing information about electron transfer and diffusional processes, together with charge separation/accumulation processes. It was employed to identify the interfacial changes after each step of the LbL formation on the electrode surface. Fig. 1B1 shows the complex plane representation of the impedance spectra acquired at −0.2 V vs. Ag/AgCl, the inset showing the equivalent circuit used to fit the spectra. The value of the potential was chosen to be −0.2 V in accordance with the electrical properties of the electrode material and the shape of the voltammograms, which become broader; indicating both layer deposition and increase in electron transfer. The magnification of Fig. 1B2 shows better the spectra of the modified Au electrodes, Au/PEDOT, Au/PEDOT/{chit$^+$(NG + GOx)}$_{n=1,2}$, with the inset showing an extra small semicircle in the high frequency region, characterizing the electrode/film interface.

The equivalent circuit, to which the spectra were fitted, consists of a cell resistance, representing the resistance of the cell and electrolyte solution (R_Ω), in series with a parallel combination of the film charge-transfer resistance (R_f) and a non-ideal capacitance (CPE$_f$), used to fit the high frequency semicircle, and a second parallel combination of the modified electrode/electrolyte solution charge transfer resistance (R_{ct}) and a double layer non-ideal capacitance (CPE$_{dl}$). The presence of the high frequency feature was attributed to the polymer and chitosan films, being seen at all modified Au electrodes. The non-ideal capacitors were represented by constant phase elements (CPE), according to the equation CPE = $[(Ci\omega)^\alpha]^{-1}$ where C is the capacitance, ω the radial frequency

Table 1
Equivalent circuit element values obtained by fitting the impedance spectra from Fig. 2B1 to the circuit from the inset.

Electrode	R_f/ Ω cm^2	CPE_f/ mF cm^{-2} s$^{\alpha-1}$	α_f	R_{ct}/ kΩ cm^2	CPE_{dl}/ μF cm^{-2} s$^{\alpha-1}$	α_{dl}
Au	–	–	–	54.4	38.2	0.85
Au/PEDOT	690	4.0	0.77	79.5	345.5	1.00
Au/PEDOT/{chit$^+$(NG + GOx)}	200	4.0	0.78	70.0	320.1	0.99
Au/PEDOT/{chit$^+$(NG + GOx)}$_2$	220	3.9	0.77	90.3	293.7	0.99

and the exponent α, which can vary between 1.0 for a perfect smooth electrode surface and 0.5 for a porous electrode, reflects surface non-uniformity, roughness and porosity.

Table 1 shows the values of each circuit component from fitting the experimental spectra to the electrical equivalent circuit. The value of the resistance of electrolyte solution and electrical contacts remains constant throughout the LbL formation process with a value $R_\Omega = 0.71\ \Omega\ cm^2$. The conducting properties of PEDOT and NG were demonstrated by the high CPE_f values which remain unchanged at 4 mF cm^{-2} s$^{\alpha-1}$, indicating that charge accumulation occurs mainly at the Au/PEDOT interface and is not influenced by the adsorption of chitosan layers. On the other hand, the film resistance values decrease from 690 Ω cm^2 for PEDOT, to 200 Ω cm^2 for the first chit(NG + GOx) layer with a slight increase for the second one. The first decrease was attributed to the presence of NG, which considerably enhances the electron transfer through the chitosan film, while the second slight increase can be explained taking into account the insulating properties of chitosan [13,21]. The average value of $\alpha_f \approx 0.77$ reflects the porosity of the PEDOT film, observed for similar electrode architectures when PEDOT was polymerized on carbon film electrodes [23]. At the electrode/electrolyte interface, values were higher for the modified Au electrodes. With PEDOT, R_{ct} increases from 54.4 kΩ cm^2 to 79.5 kΩ cm^2 and then a slight decrease was observed after deposition of the first enzymatic layer, which was attributed to the presence of NG in the layer. With the second enzymatic layer, the resistance increased up to 90.3 kΩ cm^2, following a similar tendency as R_f, though in this case Au/{chit(NG + GOx)}$_2$ has a higher value of R_{ct} than Au. The value of CPE_{dl} increased considerably from 38.2 μF cm^{-2} for bare Au, to 345.5 μF cm^{-2} s$^{\alpha-1}$ with the PEDOT layer. This suggests that the presence of the polymer leads to changes in the space charge polarization. After the adsorption of the enzymatic layers, the CPE_{dl} value was still high, but decreased slightly down to 294 μF cm^{-2} s$^{\alpha-1}$. The high values of α_{dl} of 0.99 or 1.0 for the modified Au electrodes evidence the smoothness and uniformity of the modified electrode surface at the molecular scale.

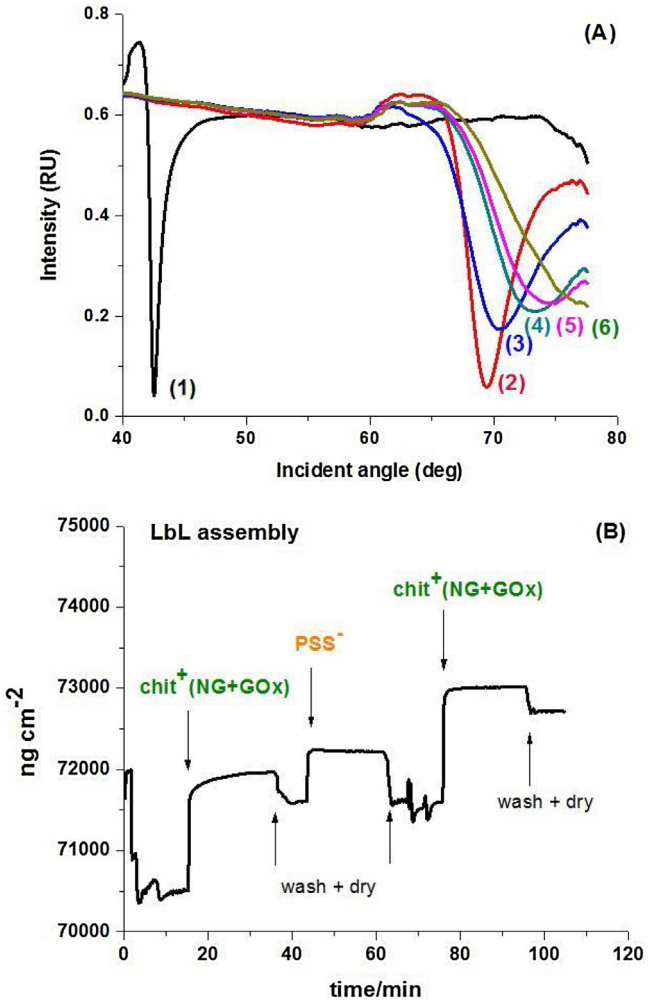

Fig. 2. PEDOT thin film deposition onto Au surface and step-by-step assembly of the LbL biosensor, in the absence of NG monitored by (A) AS-SPR. (B) FA-SPR.

3.2. Optical biosensor characterization

In biosensor applications, the SPR technique enables the study of biomolecular adsorption/desorption events at metal surfaces (e.g. gold) and allows in-situ measurements of surface coverage without any label. In this work, film growth was monitored by Angular and Fixed Angle-Surface Plasmon Resonance (AS-SPR and FA-SPR). Electrochemical-SPR (EC-SPR) can also be used for the characterization of the electrodeposition of conducting polymer thin films such as PEDOT. In EC-SPR measurements, the gold surface was used as the working electrode in a standard three-electrode electrochemical experiment. Thus, the electrochemical and optical properties are simultaneously obtained on surfaces and ultrathin films at the nanometre scale [24].

Surface plasmons are electromagnetic waves, which are very sensitive to changes at the metal surface, since the adsorption of molecules leads to small changes in the refractive index in the vicinity of the surface of a conductive thin film. The dielectric constant of each medium plays an important role: in order for the surface plasmons to exist, the dielectric constant of the metal (ε_1) must be negative, and its magnitude greater than that of the dielectric (ε_2). This condition is met in the IR-visible wavelength region for air/metal and water/metal interfaces [25,26].

For qualitative probing of PEDOT film deposition and LbL architecture formation, the angular scan mode of SPR was used. The intensity of the reflected light was recorded versus incident angle of the light, and the angle at which resonance occurs was measured (the intensity value has a minimum due to the fact that part of the light energy will turn into a plasmon surface wave traveling along the interface between the gold layer and its adjacent environment). This angle is sensitive to any change in the refractive index of the medium next to the gold surface. The modified gold surface was rinsed after each stage, in order to remove unbound molecules, followed by air drying. Fig. 2A curve (1) shows the AS-SPR spectra for a bare gold film in air. When the solution containing EDOT was introduced into the cell, the refractive index changed and curve (2) was recorded. Electrodeposition of the PEDOT film can be visualized in curve (3) when both resonance intensity and angle change. These

Table 2
Mass coverage estimation and binding for each monolayer in hydrated and dry state on Au electrode modified with PEDOT thin layer.

Layer	$m/\mu g\,cm^{-2}$ (hydrated)	$m/\mu g\,cm^{-2}$ (dry)	Binding/% (dry)
$\{chit^{+}(GOx)\}_1$	1.43 ± 0.005	1.11 ± 0.004	75.1
PSS^{-}	0.50 ± 0.010	0.01 ± 0.005	1.61
$\{chit^{+}(GOx)\}_2$	1.14 ± 0.004	1.11 ± 0.002	79.1

changes are important because they highlight the electrochromic properties of the deposited layer of PEDOT. This behaviour pattern remains for the curves which were recorded for each immobilization step of the LbL assembly onto the Au/PEDOT thin film surface: curve (4) for the first layer of $\{chit^{+}(GOx)\}$, (5) for the PSS^{-} layer and (6) for the second layer of $\{chit^{+}(GOx)\}$.

For FA-SPR measurements, a fixed angle was chosen for quantitative monitoring of the LbL assembly, such that the light falls at the specified angle of incidence, and the parallel polarised component of the evanescent field wave passes through the metal film, delocalizing the surface plasmons, the signal generated by the resonance being directly proportional to the amount of biomolecules interacting near the metal surface [27]. Molecular interactions occurred on the Au/PEDOT thin film surface as shown in Fig. 2B. For each immobilization step, the response was calculated as the difference between the SPR signal following the washing and drying step before and after sample injection. The changes in SPR signal for each immobilization step allowed a rough estimate of the corresponding average molecular surface mass uptake to be made, see Table 2. The signal obtained after the washing step was used to estimate the mass uptake in the hydrated state, while the signal obtained after drying, was used to estimate the mass uptake in the dry state. In the hydrated state a mass uptake of $1.43\,\mu g\,cm^{-2}$ was estimated for the first layer of $\{chit^{+}(GOx)\}$, and a slightly lower amount of $1.14\,\mu g\,cm^{-2}$ for the second layer, while for the dry state an equal mass uptake of $1.10\,\mu g\,cm^{-2}$ was estimated for both layers. In the case of the PSS^{-} layer, there was a big difference between the hydrated and dry states: $0.5\,\mu g\,cm^{-2}$ compared with $0.01\,\mu g\,cm^{-2}$. The mass deposited for the PSS layer in the hydrated state was almost 3 times lower than that of the enzyme layer. For each $\{chit^{+}(GOx)\}$ and PSS^{-} layer the rinsing step removes the unbound molecules, enabling the values of percentage of binding to be calculated, shown in Table 2. The maximum binding capacity, defined as the maximum layer coverage obtained under saturation conditions, was also calculated.

3.3. SEM and AFM characterization

Imaging techniques such as SEM and AFM offer insight into the physical appearance and surface characteristics of the assembled layers. Scanning electron microscopy can identify the structural morphology of the nitrogen-doped graphene. Typical SEM images of the electrode surface are shown in Fig. 3A, where Fig. 3A1 shows an overall view of the surface which presents irregularities amongst which clusters of nanoparticles and wrinkled structures (Fig. 3A2) as well as smooth areas (Fig. 3A3) can be distinguished. The wrinkled structure is due to the presence of graphene, indicating its sheet-like configuration. Steep surfaces and edges tend

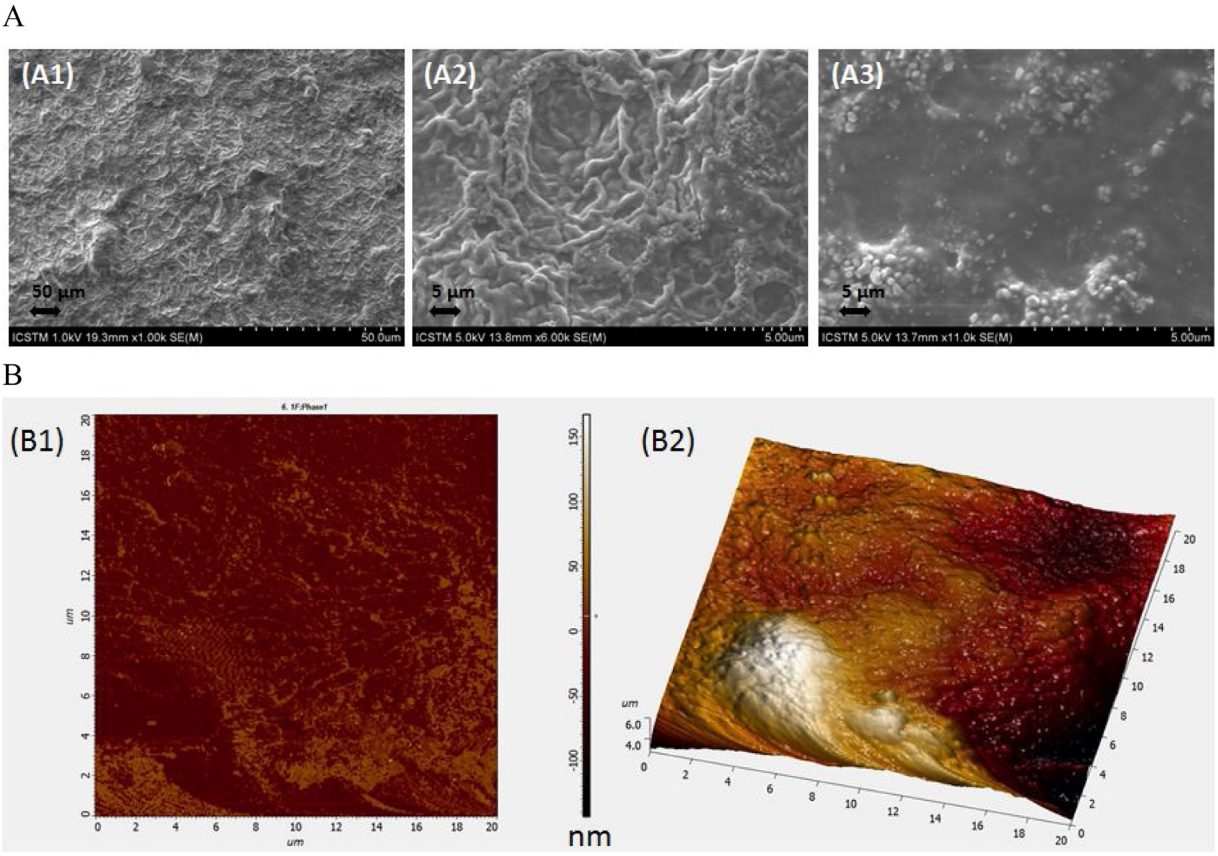

Fig. 3. (A) SEM images of Au/PEDOT/$\{chit^{+}(NG+GOx)\}_2$ electrode (A1) overall view, (A2) magnification of wrinkled structures and (A3) magnification of smooth area. (B) AFM imaging in tapping mode (B1) $20 \times 20\,\mu m$ topography-phase contrast in 2D and (B2) $20 \times 20\,\mu m$ topography in 3D, with height colour scale in nm.

to be brighter than flat surfaces, which results in images with a well-defined, three-dimensional appearance [28].

The smooth areas and clusters are also well defined by AFM imaging, illustrated in a two-dimensional (Fig. 3B1) and a three-dimensional surface profile (Fig. 3B2). AFM imaging was done in tapping mode, with the tip oscillating over the sample near its resonance frequency, meaning that the amplitude of the oscillation depends on the probe and the interaction of forces on the electrode surface (electrostatic forces) acting on the cantilever when the tip comes close to the surface, causing a change in the amplitude. This amplitude is used as the parameter that controls the height of the cantilever above the sample, providing additional information about the sample surface in the phase image that corresponds to the height image [29]. The bright colouring in Fig. 3B2 shows heights of clusters up to more than 150 nm while the dark areas correspond to smooth areas. Surface irregularities can also be seen in Fig. 3B1, where the phase contrast mode reveals the fine details of the microstructures. The estimated film thickness from the AFM results is around 70 nm.

3.4. Analytical parameters of the biosensor

3.4.1. Biosensor analytical performance for glucose detection

Fixed potential amperometry was used in order to determine the analytical performance of the newly developed label-free biosensor. In order to determine the biosensor sensitivity, a calibration curve was constructed at a fixed potential of −0.2 V vs. Ag/AgCl in 0.1 M NaPB pH 7.0 by adding increasing glucose concentrations, as shown in Fig. 4. The value of applied potential was chosen in order to minimize the effect of interferents and because it is close to the formal potential of the GOx enzymatic cofactor FAD/$FADH_2$. An anodic change in the cathodic current was recorded on each injection, indicating the occurrence of oxidation reactions. There is no mediator present in the biosensor structure, so there are two possible enzymatic mechanisms, as shown in Fig. 5. The first is based on the direct regeneration of FAD, which involves $FADH_2$ oxidation with the PEDOT-modified electrode as the electron acceptor from $FADH_2$ and glucose oxidising to gluconolactone. The second involves the use of O_2 as the electron acceptor from β-D-glucose in the presence of the enzyme, O_2 being reduced to H_2O_2 and glucose oxidised to gluconolactone [30]. The consumption of dissolved O_2 can be monitored by measuring the rate of production of H_2O_2.

At −0.2 V vs Ag/AgCl, H_2O_2 is reduced, as observed at similar electrode architectures based on PEDOT and CNT [23], but since the observed change in current was anodic, it can be deduced that the first enzymatic mechanism is dominant; this change was enhanced by the presence of NG and PEDOT. Nanomaterials exhibit high sensitivity at negative potentials, a tendency observed in the literature [31] and can be explained by their ability to regenerate the enzyme cofactor. In the presence of PEDOT polymer, enzyme regeneration was caused by a redox reaction with the oxidised form of the polymer.

The biosensor response was linear between 0.1 and 1.4 mM, with a sensitivity of 237 ± 3 μA cm^{-2} mM^{-1} and a detection limit of 41 μM. The presence of PEDOT led to an increase in sensitivity by more than one order of magnitude, compared to biosensors based on similar LbL structures developed in our previous work without PEDOT [13,21], and obtained sensitivities of ~18.6 ± 0.7 μA cm^{-2} mM^{-1} for base-functionalized graphene and acidic-functionalized CNT and 10.5 ± 0.9 μA cm^{-2} mM^{-1} for NG. We can conclude that the increase in sensitivity is due to the presence of highly conducting PEDOT.

Calibration curves were constructed at a fixed potential of −0.2 V vs. Ag/AgCl in 0.1 M NaPB pH 7.0, in order to evaluate the effect of the number of layers. The obtained sensitivities are summarized in Table 3. A configuration with two chitosan layers was considered to be the optimum due to its highest sensitivity and was used in all further experiments.

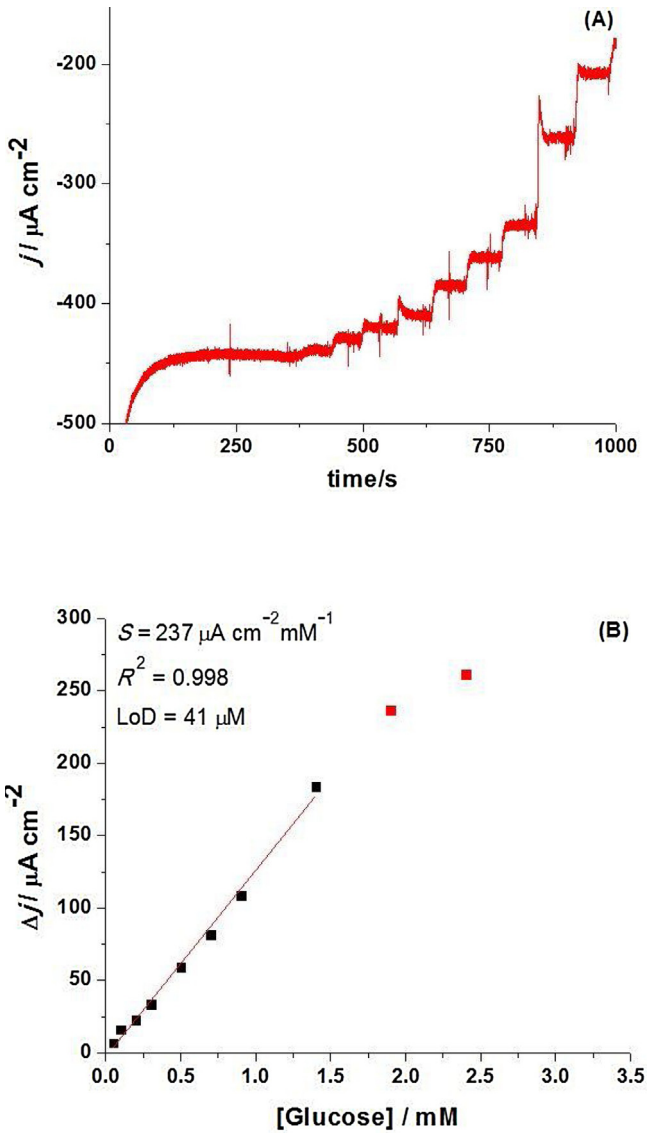

Fig. 4. (A) Fixed potential chronoamperogram for increasing concentrations of glucose and (B) corresponding calibration curve for glucose at Au/PEDOT/{chit⁺(NG + GOx)}$_2$, in 0.1 M NaPB pH 7.0, at −0.2 V vs. Ag/AgCl.

Table 3
Effect of the number of LbL layers on the biosensor sensitivity.

Layer	S/μA mM^{-1} cm^{-2}
{chit⁺(GOx)}$_1$	68.1 ± 1.37
{chit⁺(GOx)}$_2$	226.7 ± 8.02
{chit⁺(GOx)}$_3$	129.8 ± 5.18
{chit⁺(GOx)}$_4$	84.7 ± 3.40

The sensitivity of the biosensor was also tested in the presence of interferents by first recording the response to 0.3 mM glucose, followed by injecting the interferents, each with a final concentration of 0.6 mM (ratio of 1:2): dopamine, ascorbate, fructose, catechol, uric acid, sucrose, followed by two more injections corresponding to 0.3 mM glucose. In the presence of the above interferents, the biosensor lost 34% of its sensitivity, giving the value 156 ± 5 μA cm^{-2} mM^{-1} and a detection limit of 56 μM.

The long term and storage stability of the biosensor was determined by constructing one calibration plot every few days during a

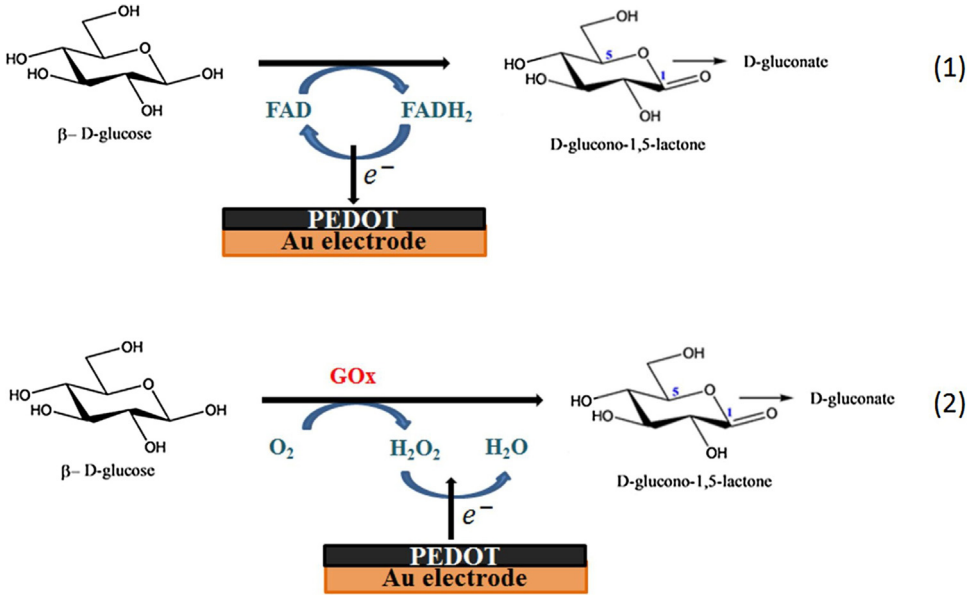

Fig. 5. GOx catalysed oxidation of glucose.

month. From the day the biosensor was prepared up to the 8th day, the sensitivity increased up to 125% of the initial value, which can be explained by rearrangement of the enzyme within the chitosan layer. On the following days it started to decrease and stabilized at 65% for the last two weeks. In between measurements, the biosensor was kept in 0.1 M NaPB, pH 7.0, at a temperature of ~4 °C. The reproducibility of the biosensors was determined by studying the activity of three sensors constructed under identical conditions, obtaining a RSD of 6.7%.

3.4.2. Biosensor analytical performance in grape wines

The biosensors were tested with wine prepared by fermentation of fresh Romanian white grape: samples E1, E2 and E3. The standard addition method was used to determine the concentration of glucose. The calculated values for glucose in the three type of wines were C_1 = 15.0 mM (2.69 g/l), C_2 = 13.1 mM (2.35 g/l) and C_3 = 12.5 mM (2.25 g/l). These values are in excellent agreement with those found in literature [32]. Analysis with independent values from the Böhringer standard spectrophotometric method led to following results $C_1 = 2.83 \pm 0.34$ g/l, $C_2 = 2.29 \pm 0.17$ g/l and $C_3 = 2.27 \pm 0.12$ g/l in agreement with our findings.

4. Conclusions

Glucose oxidase label-free biosensors based on the LbL self-assembly of the positively-charged chitosan, containing the enzyme together with NG, alternating with the negatively-charged PSS^- onto a PEDOT modified Au bulk electrode were successfully constructed. The assembly of multilayers was evidenced by CV and EIS data, both indicating an increase in the capacitance values upon first bilayer deposition and a slight decrease upon the second one, which begins to act as a diffusion barrier. Monitoring of LbL film growth by SPR, shows that the adsorbed mass significantly differs for the PSS^- and $\{chit^+(NG + GOx)\}$ layers. SEM and AFM show the influence of the presence of NG on the biosensor morphology. The amperometric biosensor response was linear in the range of 0.1–1.4 mM, with a sensitivity of $237 \pm 3\ \mu A\ cm^{-2}\ mM^{-1}$ and a detection limit of 41 μM. The presence of PEDOT significantly improved the biosensor sensitivity in comparison with previous results, where a sensitivity of $10.5 \pm 0.9\ \mu A\ cm^{-2}\ mM^{-1}$ was achieved [13]. The $\{chit^+(NG + GOx)/PSS^-\}$ bilayer-based label-free biosensor was successfully used for glucose detection in grape wines.

Acknowledgements

This work was supported by a grant of the Romanian National Authority for Scientific Research and Innovation, CNCS-UEFISCDI, project number PN-II-RU-TE-2014-4-2801. We hereby acknowledge the structural funds project PRO-DD (POS-CCE, O.2.2.1., ID 123, SMIS 2637, No. 11/2009) for providing the infrastructure used in this work. We also thank Fundação para a Ciência e a Tecnologia (FCT), Portugal project UID/EMS/00285/2013 (co-financed by the European Community Fund FEDER) and M.M.B. thanks FCT for a postdoctoral fellowship SFRH/BPD/72656/2010.

For AFM and SEM imaging we are grateful to Dr. Ioana Daniela Dulama and PhDs Eng. Ioan Alin Bucurica, Valahia University of Targoviste, Multidisciplinary Scientific and Technological Research Institute.

References

[1] A. Sassolas, L.J. Blum, B.D. Leca-Bouvier, Immobilization strategies to develop enzymatic biosensors, Biotechnol. Adv. 30 (2012) 489–511.
[2] W. Zhao, J.J. Xu, H.Y. Chen, Electrochemical biosensors based on layer-by-layer assemblies, Electroanalysis 18 (2006) 1737–1748.
[3] W. Putzbach, N.J. Ronkainen, Immobilization techniques in the fabrication of nanomaterial-based electrochemical biosensors: a review, Sensors 13 (2013) 4811–4840.
[4] M. Michel, V. Toniazzo, D. Ruch, V. Ball, Deposition mechanisms in layer-by-layer or step-by-step deposition methods: from elastic and impermeable films to soft membranes with ion exchange properties, ISRN Mater. Sci. 2012 (2012) 13 (701695).
[5] E.M. Pinto, M.M. Barsan, C.M.A. Brett, Mechanism of formation and construction of self-assembled myoglobin/hyaluronic acid multilayer films: an electrochemical QCM, impedance, and AFM study, J. Phys. Chem. B 114 (46) (2010) 15354–15361.
[6] J.S. Graça, R.F. de Oliveira, M.L. de Moraes, M. Ferreira, Amperometric glucose biosensor based on layer-by-layer films of microperoxidase-11 and liposome-encapsulated glucose oxidase, Biochemistry 96 (2014) 37–42.
[7] X. Kang, J. Wang, H. Wu, I.A. Aksay, J. Liu, Y. Lin, Glucose Oxidase-graphene-chitosan modified electrode for direct electrochemistry and glucose sensing, Biosens. Bioelectron. 25 (2009) 901–905.
[8] W. Lian, S. Liu, J. Yu, X. Xing, J. Li, M. Cui, J. Huang, Electrochemical sensor based on gold nanoparticles fabricated molecularly imprinted polymer film at chitosan-platinum nanoparticles/graphene-gold nanoparticles double nanocomposites modified electrode for detection of erythromycin, Biosens. Bioelectron. 38 (2012) 163–169.

[9] S. Liu, J. Ou, Z. Li, S. Yang, J. Wang, Layer-by-layer assembly and tribological property of multilayer ultrathin films constructed by modified graphene sheets and polyethyleneimine, Appl. Surf. Sci. 258 (2012) 2231–2236.
[10] M. Ma, Z. Miao, D. Zhang, X. Du, Y. Zhang, C. Zhang, J. Lin, Q. Chen, Highly-ordered perpendicularly immobilized FWCNTs on the thionine monolayer-modified electrode for hydrogen peroxide and glucose sensors, Biosens. Bioelectron. 64 (2015) 477–484.
[11] M. Gerard, A. Chaubey, B.D. Malhorta, Application of conducting polymers to biosensors, Biosens. Bioelectron. 17 (2002) 354–359.
[12] V. Serafin, L. Agüí, P. Yáñez-Sedeño, J.M. Pingarrón, A novel hybrid platform for the preparation of disposable enzyme biosensors based on poly(3,4-ethylenedioxythiophene) electrodeposition in a ionic liquid medium onto gold nanoparticles-modified screen-printed electrodes, J. Electroanal. Chem. 656 (2011) 152–158.
[13] M.M. Barsan, M. David, M. Florescu, L. Ţugulea, C.M.A. Brett, A new self-assembled layer-by-layer biosensor based on chitosan biopolymer entrapped enzyme with nitrogen doped grapheme, Bioelectrochemistry 99 (2014) 46–52.
[14] M.E. Ghica, R. Pauliukaite, O. Fatibello-Filho, C.M.A. Brett, Application of functionalised carbon nanotubes immobilised into chitosan films in amperometric enzyme biosensors, Sens. Actuator B-Chem. 142 (2009) 308–315.
[15] A. Wisitsoraat, S. Pakapongpan, C. Sriprachuabwong, D. Phokharatkul, P. Sritongkham, T. Lomas, A. Tuantranont, Graphene-PEDOT:PSS on screen printed carbon electrode for enzymatic biosensing, J. Electroanal. Chem. 704 (2013) 208–213.
[16] D.A.C. Brownson, C.E. Banks, Graphene electrochemistry: an overview of potential applications, Analyst 135 (2010) 2768–2778.
[17] D. Geng, S. Yang, Y. Zhang, J. Yana, J. Liu, R. Li, et al., Nitrogen doping effects on the structure of graphene, Appl. Surf. Sci. 257 (2011) 9193–9198.
[18] A. Baba, M.K. Park, R.C. Advincula, W. Knoll, Simultaneous surface plasmon optical and electrochemical investigation of layer-by-layer self-assembled conducting ultrathin polymer films, Langmuir 18 (2002) 4648–4652.
[19] R.F. Dutra, R.K. Mendes, V.L. da Silva, L.T. Kubota, Surface plasmon resonance immunosensor for human cardiac troponin T based on self-assembled monolayer, J. Pharm. Biomed. Anal. 43 (2007) 1744–1750.
[20] S. Kakhki, M.M. Barsan, E. Shams, C.M.A. Brett, Development and characterization of poly(3,4-ethylenedioxythiophene)-coated poly(methylene blue)-modified carbon electrodes, Synth. Met. 161 (2012) 2718–2726.
[21] M. David, M.M. Barsan, M. Florescu, C.M.A. Brett, Acidic and basic functionalized carbon nanomaterials as electrical bridges in enzyme loaded chitosan/poly(styrene sulfonate) self-assembled layer-by-layer glucose biosensors, Electroanalysis 27 (2015) 2139–2149.
[22] Y.-C. Yang, S.-W. Dong, T. Shen, C.-X. Jian, H.-J. Chang, Y. Li, J.-X. Zhou, Amplified immunosensing based on ionic liquid-doped chitosan film as a matrix and Au nanoparticle decorated graphene nanosheets as labels, Electrochim. Acta 56 (2011) 6021–6025.
[23] V. Pifferi, M.M. Barsan, M.E. Ghica, L. Falciola, C.M.A. Brett, Synthesis characterization and influence of poly(brilliant green) on the performance of different electrode architectures based on carbon nanotubes and poly(3,4-ethylenedioxythiophene), Electrochim. Acta 98 (2013) 199–207.
[24] A. Baba, P. Taranekar, R.R. Ponnapati, W. Knoll, R.C. Advincula, Electrochemical surface plasmon resonance (EC-SPR) and waveguide enhanced glucose biosensing with N-alkylaminated polypyrrole/glucose oxidase multilayers, ACS Appl. Mater. Interfaces 2 (2010) 2347–2354.
[25] S. Zeng, D. Baillargeat, H.P. Ho, K.T. Yong, Nanomaterials enhanced surface plasmon resonance for biological and chemical sensing applications, Chem. Soc. Rev. 43 (2014) 3426–3452.
[26] R.J. Green, R.A. Frazier, K.M. Shakesheff, M.C. Davies, C.J. Roberts, S.J.B. Tendler, Surface plasmon resonance analysis of dynamic biological interactions with biomaterials, Biomat 21 (2000) 1823–1835.
[27] I.N. Serdyuk, N.R. Zaccai, J. Zaccai, Methods in Molecular Biophysics: Structure, Dynamics Function, Cambridge University Press, 2007.
[28] L. Frank, M. Hovorka, Š. Mikmeková, E. Mikmeková, I. Müllerová, Z. Pokorná, Scanning electron microscopy with samples in an electric field, Materials 5 (2012) 2731–2756.
[29] N.A. Geisse, AFM and combined optical techniques, Mater. Today 12 (7-8) (2009) 40–45.
[30] P.-C. Nien, T.-S. Tung, K.-C. Ho, Amperometric glucose biosensor based on entrapment of glucose oxidase in a poly(3,4-ethylenedioxythiophene) film, Electroanalysis 18 (2006) 1408–1415.
[31] M.M. Barsan, K.P. Prathish, X. Sun, C.M.A. Brett, Nitrogen doped graphene and its derivatives as sensors and efficient direct electron transfer platform for enzyme biosensors, Sens. Actuator B-Chem. 203 (2014) 579–587.
[32] P.P. Minnaar, N. Ntushelo, Z. Ngqumba, V. van Breda, N.P. Jolly, Effect of Torulaspora delbrueckii yeast on the anthocyanin and flavanol concentrations of Cabernet franc and Pinotage wines, South Afr. J. Enol. Vitic. 36 (1) (2015) (Stellenbosch).

Biographies

Melinda David is a Ph. D. student at the Doctoral School of Biophysics, Faculty of Physics, University of Bucharest, Romania. Her Ph. D. theme as well as research interest is about the fabrication of several types of biosensors and their characterization using different methods; the main activities being: biosensor development, and their characterization using optical and electrochemical methods, surface imaging and latest, their application in real samples.

Madalina Maria Barsan received her Ph. D. degree at University of Coimbra, Portugal, in 2011, where she is currently a Postdoctoral Researcher. Her research interests include the development and characterization of new nanostructured electrode materials and methods for biomolecule immobilization for new electrochemical (bio)sensors and their application in the environmental, health, food and pharmaceutical areas.

Christopher Brett is a professor of chemistry at the University of Coimbra, Portugal. His research interests include new nanostructured electrode materials and modified electrode surfaces, electrochemical sensors and biosensors, electroactive polymers, corrosion and its inhibition, and applications of electrochemistry in the environmental, health, food and pharmaceutical areas. He was President of the International Society of Electrochemistry (ISE) in 2007-8. He is an elected member of the Bureau of the International Union of Pure and Applied Chemistry (IUPAC) for the period 2012-19 and a member of the IUPAC Executive Committee 2016-17. He was President of the Physical and Biophysical Chemistry Division of IUPAC in 2006-7, is a former Chairman of the IUPAC Electrochemistry Commission, and was President of the Analytical Division of the Portuguese Chemical Society (2003-5). He is a Fellow of the Royal Society of Chemistry. He is also Director of the Electroanalysis and Corrosion Laboratory, Instituto Pedro Nunes, Coimbra, the technological innovation link between the University of Coimbra and the industrial sector. His research activity is documented by more than 275 papers and 20 chapters in multi-author books, and has been presented in many conferences and invited lectures. He is co-author of 2 undergraduate/graduate textbooks "*Electrochemistry. Principles, methods and applications*", 1993, and "*Electroanalysis*", 1998, both Oxford University Press.

Monica Florescu received her Ph.D. in Biophysics from Faculty of Physics of the University of Bucharest, Romania. She had received doctoral scholarships to work on sensors and biosensors development (DAAD – German Academic Exchange Service, Erasmus) and postdoctoral fellowship at University of Wisconsin-Milwaukee, USA for *in vivo* study of biological tissues using dielectric spectroscopy techniques. Currently she is Assistant Professor of Biophysics and Medical Physics at the Department of Fundamental, Prophylactic, and Clinical Disciplines, Faculty of Medicine, Transylvania University of Brasov, Romania. Her current research interests include nanostructured and modified electrode surfaces, development, characterization and evaluation of (bio)sensors for active biological compounds and contaminants detection and their applications for biomedical, food and environment using label-free methods like electrochemistry (voltammetry, amperometry, electrochemical impedandace spectroscopy) and optical spectroscopy (surface plasmon resonance spectroscopy, UV-VIS, fluorescence).